Article

Discovery Medicine 2025; 37(199): 1510–1519
https://doi.org/10.24976/Discov.Med.202537199.131

Micheliolide Induces Ferroptosis to Restrain the Malignant Phenotype of Non-Small Cell Lung Cancer Cells

Hong Lv[1,†], Tiefeng Qiu[2,3,†], Qinyu Xu[2,3,*]

[1]Department of Respiratory Medicine, Affiliated Hospital of Nanjing University of Chinese Medicine, Taicang Hospital of Traditional Chinese Medicine, 215499 Taicang, Jiangsu, China
[2]Department of Respiratory Medicine, Wujin Hospital Affiliated With Jiangsu University, 213003 Changzhou, Jiangsu, China
[3]The Wujin Clinical College of Xuzhou Medical University, 213003 Changzhou, Jiangsu, China
*Correspondence: 13861254250@163.com (Qinyu Xu)
[†]These authors contributed equally.
Published: 20 August 2025

Background: Ferroptosis is an iron-dependent form of regulated cell death, which offers therapeutic potential in non-small cell lung cancer (NSCLC). This study aimed to evaluate whether Micheliolide (MCL) induces ferroptosis in NSCLC cells via the nuclear factor erythroid 2-related factor 2 (Nrf2) signaling pathway.

Methods: H1299 cells were treated with different concentrations of MCL. Cellular assays, including the Cell Counting Kit-8 (CCK-8), colony formation, scratch test, and Transwell, were used to evaluate the viability, proliferation, migration, and invasion of the cells. Ferroptosis-related indicators (reactive oxygen species (ROS), malondialdehyde (MDA), glutathione (GSH), Fe^{2+}) and protein expression (Nrf2, glutathione peroxidase 4 (GPX4), Acyl-CoA Synthetase Long-Chain Family Member 4 (ACSL4), Transferrin Receptor 1 (TFR1) were assessed via flow cytometry, biochemical assays, and Western blot. Additionally, Nrf2-specific activator (tert-butylhydroquinone (tBHQ)) and ferroptosis inhibitors (Fer-1) were used to verify the involvement of this pathway.

Results: MCL inhibited proliferation, migration, and invasion of H1299 cells in a dose-dependent manner and induced ferroptosis as evidenced by elevated ROS, MDA, and Fe^{2+} levels, and reduced GSH concentration. Western blot analysis revealed significantly increased ACSL4 and TFR1 and decreased Nrf2 and GPX4 expression. These MCL-induced effects were reversed by tBHQ or Fer-1, confirming the involvement of Nrf2.

Conclusions: MCL induces ferroptosis in NSCLC cells by suppressing the Nrf2 pathway. Targeting Nrf2 may enhance the anticancer efficacy of Micheliolide, offering new therapeutic insights for NSCLC.

Keywords: Micheliolide; non-small cell lung cancer; Nrf2, ferroptosis; cell proliferation; invasion; migration

Introduction

Lung cancer remains the leading cause of cancer-related deaths worldwide [1]. Histologically, lung cancer is classified into non-small cell lung cancer (NSCLC) and small cell lung cancer (SCLC), with NSCLC representing approximately 85% and SCLC the remaining 15% of all cases [2]. Conventional therapeutic approaches for lung cancer include surgical interventions, chemotherapy and radiation therapy [3]. In recent years, the development of molecular targeted therapies and immunotherapy has expanded the range of treatment options [4]. Although chemotherapeutic agents are widely used to induce apoptosis in tumor cells, the increasing incidence of drug resistance highlights the need to explore alternative cell death mechanisms as potential options for novel anticancer therapies [2].

Ferroptosis is a unique form of cell death characterized by iron-dependent lipid peroxidation, offering a promising therapeutic target [5–7]. It is defined by iron accumulation, elevated malondialdehyde (MDA) levels, and compromised mitochondrial integrity. The excessive production of reactive oxygen species (ROS) triggers ferroptosis by inducing oxidative stress and subsequent cellular damage, contributing to the pathogenesis of various diseases, including cancer [8–12]. This process is regulated by the balance between cellular redox status and lipid metabolism, with crucial involvement of molecules such as glutathione (GSH) peroxidase 4 (GPX4), iron metabolism-related proteins, and the nuclear factor erythroid 2-related factor 2 (Nrf2) pathway [13]. Under normal conditions, Nrf2 is sequestered in the cytoplasm by its repressor, Kelch-like Electrophile Carrier Homolog (ECH)-associated protein 1 (KEAP1) [14,15]. In response to oxidative stress, Nrf2 is

activated, translocates to the nucleus, and leads to expression of antioxidant response elements (ARE)-driven target genes, thereby creating a cellular environment that supports NSCLC cell survival and proliferation [13–17]. Therefore, targeting Nrf2 with small molecule inhibitors may offer a viable strategy to sensitize NSCLC cells to ferroptosis.

Natural products are increasingly recognized as valuable sources for the development of novel anticancer agents, particularly due to their ability to enhance tumor susceptibility to existing therapies. Micheliolide (MCL), a natural compound, has demonstrated significant therapeutic potential in treating inflammation and various cancers, including mucoepidermoid carcinoma (MEC) and head and neck squamous cell carcinoma (HNSCC) [18–20]. Research indicates that Micheliolide enhances the radiosensitivity of p53-deficient NSCLC and overcomes platinum-based chemotherapy resistance in NSCLC cells [21]. However, its overall therapeutic efficacy against NSCLC remains to be fully elucidated.

Therefore, this study aimed to explore the anticancer effects and underlying mechanisms of Micheliolide, with the goal of developing novel therapeutic approaches for lung cancer. We hypothesized that Micheliolide triggers ferroptosis in NSCLC cells by modulating ROS levels, lipid peroxidation, and the Nrf2 signaling pathway. To validate this hypothesis, we conducted a comprehensive *in vitro* analysis of Micheliolide's anticancer effects, evaluating its impact on cell proliferation, migration, and invasion, alongside its modulation of ferroptosis-related biomarkers. Furthermore, we examined the involvement of the Nrf2 pathway in Micheliolide-induced ferroptosis, providing deeper insights into its anticancer mechanisms. Our findings add to the growing body of evidence supporting the anticancer therapeutic potential of Micheliolide, particularly in the context of NSCLC treatment.

Materials and Methods

Cell Culture

The human NSCLC cell line H1299 (p53-null) was obtained from the National Collection of Authenticated Cell Cultures (Catalog No. TCHu160, Chinese Academy of Sciences, Shanghai, China). The supplier authenticated the cell lines using routine short tandem repeat (STR) profiling. To minimize genetic drift, experiments were performed using cells within 10 passages. The cells were maintained in Roswell Park Memorial Institute (RPMI) 1640 medium (GE Healthcare Life Sciences, Logan, UT, USA) containing 100 U/mL penicillin (Gibco, Carlsbad, CA, USA), 100 µg/mL streptomycin (Gibco, Carlsbad, CA, USA), and 10% fetal bovine serum (FBS) (GE Healthcare Life Sciences, Logan, UT, USA). Under normoxic conditions, incubation was conducted at 37 °C in a humidified environment containing 95% air and 5% CO_2. All cell cultures were found negative for mycoplasma contamination. Micheliolide (obtained from Wuhan ChemFaces Biochemical, Wuhan, China) was dissolved in DMSO before use.

Isolation of Cytoplasm and Nucleus

Nuclear and cytoplasmic fractions were isolated using the Nuclear and Cytoplasmic Extraction Kit (Beyotime, Shanghai, China) following the manufacturer's protocols. Briefly, cells were harvested, washed with cold PBS, and resuspended in homogenization buffer containing Tris-HCl, sucrose, EDTA, and protease inhibitors. The suspension was homogenized on ice using a Dounce homogenizer to disrupt the plasma membrane while preserving nuclear integrity. The homogenate was centrifuged at 600 $\times g$ for 10 minutes at 4 °C to pellet the nuclei and any intact cells. The resulting supernatant, containing the cytoplasmic components and organelles, underwent an additional centrifugation at 10,000 $\times g$ for 20 minutes at 4 °C to isolate the cytosol fraction. The nuclear pellet was washed, followed by another round of centrifugation at 600 $\times g$ to ensure purity, and the resulting pellet was collected as the nuclear fraction. All procedures were performed on ice in the presence of protease inhibitors.

Cell Viability Test

To evaluate the cytotoxic effect of MCL on NSCLC cells, H1299 cells were treated with various concentrations of MCL (0, 5, 10, 20 µM) for 24 hours. Cell viability was assessed using the Cell Counting Kit-8 (CCK-8) (Catalog No. K1018, ApexBio, Houston, TX, USA). Following treatment, each well was supplemented with 200 µL of CCK-8 solution and incubated at 37 °C for one hour. Absorbance was measured at 450 nm using a microplate reader (Varioskan Flash, Thermo Fisher, Waltham, MA, USA). The relative cell viability (%) was calculated using the following formula:

$$\text{Cell viability (\%)} = \frac{\text{ODtreatmert} - \text{ODblank}}{\text{ODcontrol} - \text{ODblank}} \times 100\%$$

Colony Formation Assay

H1299 cells were seeded in 6-well plates (Corning Incorporated, Corning, NY, USA) at a density of 500 cells per well. After allowing 24 hours for cell adhesion, the cells were treated with Micheliolide alone or in combination with either 10 µM tert-butylhydroquinone (tBHQ), an activator of Nrf2-specific and incubated for 14 days. The cells were then fixed with 4% paraformaldehyde for 30 minutes at room temperature, followed by three washes with PBS. The fixed cells were subsequently stained with crystal violet (Beijing Solarbio Science & Technology Co., Ltd., Beijing, China) for 30 minutes at room temperature. Excess crystal violet was removed by washing with PBS, and colonies containing 50 or more cells were counted following a previously described protocol [22].

Wound Healing Assay

H1299 cells were incubated with MCL, with or without 10 μM tBHQ (Catalog No. 112941, Sigma-Aldrich, St. Louis, MO, USA), in DMEM supplemented with 0.1% bovine serum albumin for 24 hours. The cells were uniformly seeded into 6-well plates. A scratch was made in the cell monolayer using a 200 μL pipette tip. Cells were then cultured in serum-free medium, and images of the wound area were captured at 0 and 24 hours after scratching. Wound closure was quantitatively analyzed using ImageJ software (version 1.53t; National Institutes of Health, Bethesda, MD, USA), and the wound healing rate was calculated using the formula: [(wound area at 0 h – wound area at 24 h)/wound area at 0 h] $\times$ 100%.

Transwell Assay

Cell invasion was assessed using a Transwell assay. H1299 cells suspension (150 μL) was seeded into the upper chamber of a Transwell insert pre-coated with Matrigel (Becton, Dickinson and Company, Franklin Lakes, NJ, USA). The lower chamber was filled with 600 μL of medium containing FBS. After 24 hours of incubation, cells that had invaded the Matrigel and adhered to the lower side of the membrane were fixed with paraformaldehyde (4%) and stained with crystal violet dye, and the stained cells were counted using a microscope.

Flow Cytometry

Following MCL and ferrostatin-1 (Fer-1), ferroptosis inhibitor (Cat. No. SML0583, Sigma-Aldrich St. Louis, MO, USA) treatment, approximately 1×10^6 cells in the logarithmic growth phase were collected and digested. After washing three times with PBS, cells were incubated with 10 μM BODIPY 581/591 C11 (Catalog No. D3861, Thermo Fisher Scientific, Waltham, MA, USA) at 37 °C to determine lipid ROS levels. After incubation, the cells were analyzed by flow cytometry using a BD FACSCanto II cytometer (Becton, Dickinson and Company, Franklin Lakes, NJ, USA). The cells were examined using the Fluorescein Isothiocyanate (FITC) channel, and lipid ROS levels were quantified based on mean fluorescence intensity (MFI) using FlowJo software (Version 10.8.1, BD Biosciences, Ashland, OR, USA).

Measurement of Malondialdehyde, Glutathione, and Iron Content

Cells were seeded into 6-well plates at a density of 1×10^6 cells/well and allowed to adhere for 24 hours. MDA levels were measured at 532 nm using a lipid oxidation test kit (Catalog No. S0131S, Beyotime, Beijing, China), GSH levels at 412 nm using a GSH assay kit (Catalog No. ab65322, Abcam, Cambridge, UK), and Fe^{2+} levels at 593 nm using the Iron Ion Colorimetric Assay Kit (Catalog No. E1042, Applygen, Beijing, China). Each assay was performed in triplicate, and quantitative analysis was conducted using standard curves according to the manufacturer's protocols. Absorbance for all assays was determined using a microplate reader.

Western Blot Analysis

Protein samples were separated using SDS-PAGE (8% gel) and subsequently transferred onto PVDF membranes. After blocking with 8% skim milk for 2 hours, the membranes were incubated overnight at 4 °C with primary antibodies against Nrf2 (Servicebio, Wuhan, China; Catalog No. GB113808-100; 1:1000), GPX4 (Servicebio, Wuhan, China; Catalog No. GB115275-100; 1:1000), Acyl-CoA Synthetase Long-Chain Family Member 4 (ACSL4) (Servicebio, Wuhan, China; Catalog No. GB115608-100; 1:1000), Transferrin Receptor 1 (TFR1) (Merck Millipore, Burlington, MA, USA; Catalog No. MABC1765; 1:1000), GAPDH (Servicebio, Wuhan, China; Catalog No. GB11002-100; 1:2000), and Histone H3 (Servicebio, Wuhan, China; Catalog No. GB11026-100; 1:1000). The next day, membranes were incubated with appropriate HRP-conjugated secondary antibodies (Servicebio, Wuhan, China; Catalog No. GB23303; 1:10,000) for 1 hour at room temperature. Protein bands were visualized using an ECL Kit (Abcam, Cambridge, MA, USA; Catalog No. ab65623) and imaged using the Tanon 5200 Multi Chemiluminescent Imaging System (Cat. No. 5200, Shanghai, China). Band intensities were quantified using ImageJ software and normalized to Glyceraldehyde-3-phosphate dehydrogenase (GAPDH) or Histone H3 as internal loading controls.

Statistical Analysis

Experimental data were analyzed using SPSS 20.0 software (IBM Corp., Armonk, NY, USA), and outcomes were expressed as mean $\pm$ standard deviation (SD). All experiments were independently repeated three times, and the data were recorded as the means of three biological replicates. To assess differences among multiple groups, one-way analysis of variance (ANOVA) was used to effectively control the family-wise error rate. Post hoc analyses were selected based on the nature of the comparisons: Dunnett's test was applied when comparing each experimental group to a single control, while Tukey's test was used for multiple group comparisons without a specific control. A p-value of <0.05 was deemed statistically significant.

Results

Micheliolide Inhibits Proliferation, Migration, and Invasion of H1299 Cells

Micheliolide significantly inhibited the viability of NSCLC cells in a dose-dependent manner at concentrations of 5, 10, and 20 μM. Specifically, treatment with 20 μM Micheliolide led to a significant reduction in the viability of H1299 cells after 24 hours ($p < 0.01$, Fig. 1A). CCK-8 assay demonstrated that Micheliolide induces a dose-

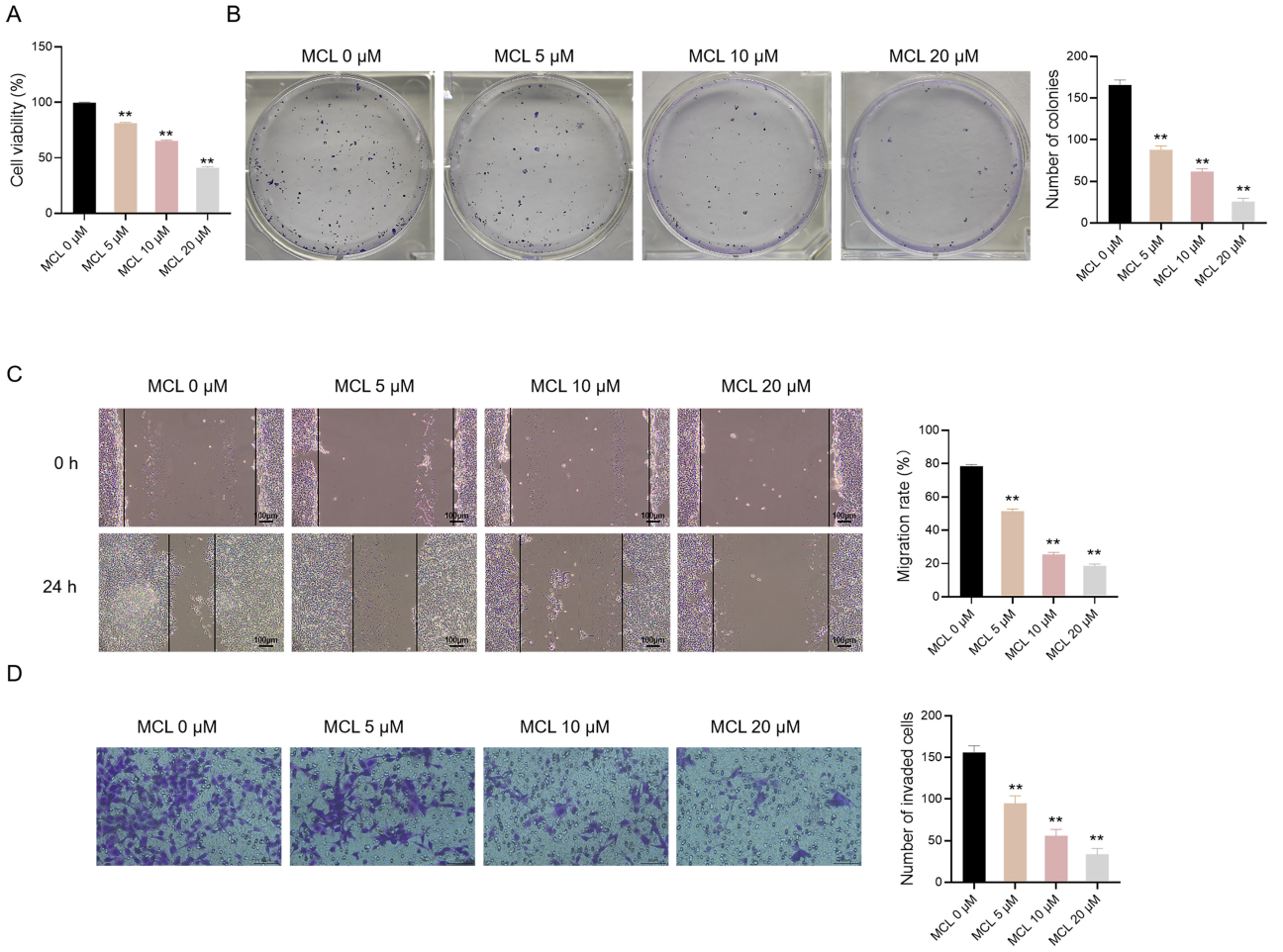

Fig. 1. The impact of Micheliolide on viability, proliferation, invasion, and migration of H1299 cells. CCK-8 assay (A) was utilized to evaluate cell viability, the colony formation assay (B) to assess proliferation, and the wound healing assay (C) and Transwell assay (D) to examine migration and invasion abilities, respectively. $^{**}p < 0.01$ vs. untreated cells (0 μM). Each experiment was independently performed in triplicate (n = 3). MCL, Micheliolide; CCK-8, Cell Counting Kit-8.

dependent reduction in cell viability. Additionally, its impact on cell proliferation, migration, and invasion was also assessed. Micheliolide significantly reduced the colony formation in H1299 cells, with the most pronounced inhibition observed at 20 μM after 14 days of incubation ($p < 0.01$, Fig. 1B).

The migration ability of H1299 cells was progressively decreased with increasing concentrations of Micheliolide, with a significant reduction observed at 20 μM after 24 hours ($p < 0.01$, Fig. 1C). Transwell assays further confirmed that Micheliolide significantly impaired cell invasion in a concentration-dependent manner, significantly suppressed cell invasion, with significant inhibition observed at 10 μM ($p < 0.01$, Fig. 1D). These findings indicate that Micheliolide decreases the viability, proliferation, migration, and invasion of H1299 cells in a concentration-dependent manner.

Micheliolide Induces Ferroptosis in H1299 Cells

Ferroptosis is a form of non-apoptotic cell death which is characterized by intracellular iron accumulation and leads to increased lipid peroxidation and ROS production. A key feature of ferroptosis is the downregulation of GPX4, an essential enzyme involved in cellular antioxidant defense [23]. In this study, we investigated key biomarkers of ferroptosis, including ROS, MDA, GSH, and ferrous ions (Fe^{2+}), as well as the expression of ferroptosis-associated proteins GPX4, ACSL4, and TFR1, to assess whether Micheliolide induces ferroptosis. Micheliolide treatment led to a significant increase in ROS levels (Fig. 2A), elevated MDA (Fig. 2B), and higher Fe^{2+} concentrations (Fig. 2D), accompanied by a reduction in GSH levels (Fig. 2C). Furthermore, Micheliolide significantly upregulated the expression of ferroptosis-associated proteins ACSL4 and TFR1 ($p < 0.01$), while downregulating GPX4 expression compared to the control group ($p < 0.01$, Fig. 2E,F). Importantly, these ferroptosis-associated

effects were reversed by Fer-1, a ferroptosis inhibitor, indicating that Micheliolide-induced ferroptosis is a modifiable cellular process (Fig. 2A–F).

Micheliolide Inhibits the Activation of the Nrf2 Pathway in H1299 Cells

To elucidate the role of Nrf2 in Micheliolide-induced ferroptosis, we assessed the changes in the Nrf2 pathway in H1299 cells exposed to Micheliolide. The results demonstrated a significant reduction in Nrf2 expression in both the cytoplasm and nucleus following Micheliolide treatment. Exposure to 5 μM or higher concentrations of Micheliolide resulted in a notable dose-dependent decrease in Nrf2 localization across these cellular compartments (Fig. 3A,B). These results indicate that the Nrf2/GSH/GPX4 pathway may play a crucial role in mediating Micheliolide-induced ferroptosis in NSCLC.

Nrf2 Activation Counteracts Micheliolide-Induced Ferroptosis in H1299 Cells

To further validate the impact of Nrf2 on Micheliolide-induced ferroptosis, we utilized the Nrf2-specific activator tBHQ to explore the interaction between Nrf2 and ferroptosis under Micheliolide exposure. tBHQ pre-treatment significantly elevated Nrf2 expression in both the nucleus and cytoplasm ($p < 0.01$, Fig. 4A), restoring levels comparable to those observed in the control group. This activation of Nrf2 mitigated Micheliolide-induced ferroptosis, as evidenced by a significant reduction in ROS levels compared to Micheliolide treatment alone (Fig. 4B). Furthermore, tBHQ pre-treatment decreased MDA and intracellular iron levels while markedly increasing GSH levels compared to Micheliolide treatment alone (Fig. 4C–E). Additionally, tBHQ pre-treatment significantly upregulated GPX4 expression and downregulated ferroptosis-related proteins ACSL4 and TFR1, restoring their levels close to those of the control group (Fig. 4F,G). Overall, these findings suggest that Nrf2 activation by tBHQ effectively counteracts Micheliolide-induced ferroptosis, highlighting the antagonistic role of Nrf2 in this cell death pathway.

Nrf2 Activation Promotes Proliferation, Migration, and Invasion of Micheliolide-Treated H1299 Cells

After establishing that tBHQ-induced Nrf2 activation suppresses Micheliolide-induced ferroptosis, we further investigated how Micheliolide affects NSCLC proliferation, migration, and invasion through Nrf2 modulation. H1299 cells were pre-treated with the Nrf2 activator tBHQ prior to assessing cell viability using the CCK-8 assay. The findings revealed a significant reduction in Micheliolide-induced cell death following tBHQ pre-treatment ($p < 0.01$, Fig. 5A). It was observed that tBHQ pre-treatment not only preserved cell viability but also promoted proliferation, with colony formation levels nearly restored to those of the control group ($p < 0.01$, Fig. 5B). Scratch wound assays indicated that tBHQ pre-treatment effectively restored the migration ability of Micheliolide-treated H1299 cells ($p < 0.01$, Fig. 5C). Furthermore, Transwell assays confirmed a substantial reversal of Micheliolide-induced invasion impairment ($p < 0.01$, Fig. 5D). Collectively, these findings provide compelling evidence that Micheliolide impairs NSCLC cell viability, proliferation, migration, and invasion by targeting Nrf2 to induce ferroptosis.

Discussion

This study investigates the therapeutic potential of Micheliolide in NSCLC by assessing its ability to induce ferroptosis, a regulated form of non-apoptotic cell death characterized by iron-dependent lipid peroxidation [6,7]. Our findings provided compelling evidence supporting Micheliolide as a potent inducer of ferroptosis in NSCLC therapy, exhibiting significant antitumor effects *in vitro*. Micheliolide effectively suppressed the proliferation, migration, and invasion of H1299 lung cancer cells in a concentration-dependent manner, aligning with previous studies underscoring its anti-cancer effects in various cancer cell lines [24–26]. The ability of Micheliolide to inhibit tumor growth and metastasis suggests its therapeutic potential in NSCLC treatment.

A key finding in our study was the identification of ferroptosis as a potential mechanism underlying Micheliolide-induced cytotoxicity in NSCLC cells. Micheliolide treatment led to increased levels of ROS, lipid peroxidation, and intracellular iron, the hallmark indicators of ferroptosis. Excessive ROS further drives lipid peroxidation, ultimately oxidizing into malondialdehyde [27]. In this study, Micheliolide treatment significantly enhanced MDA production in H1299 cells, further confirming ferroptosis induction.

Nrf2 is a key transcription factor that regulates the expression of numerous genes involved in mitigating oxidative stress and subsequent lipid peroxidation by reducing ROS levels. Notably, Nrf2 governs the synthesis of GSH, an essential antioxidant enzyme that relies on NADPH to regenerate its reduced form from the oxidized state. GPX4 is another key enzyme that protects cells from ferroptosis by converting cytotoxic lipid peroxides into non-toxic lipid alcohols [13]. Hence, inhibiting Nrf2 is anticipated to trigger ferroptosis in NSCLC cells. We investigated whether Micheliolide induces ferroptosis in NSCLC cells through suppression of the Nrf2 pathway. Unsurprisingly, Micheliolide treatment remarkably downregulated the expression of Nrf2, GSH and GPX4. This inhibition of Nrf2 signaling sensitizes cells to ferroptosis, making them more vulnerable to oxidative damage induced by Micheliolide. Conversely, Fer-1, a selective ferroptosis inhibitor, has been shown to hinder excessive ROS production and abolish ferroptosis [7,28]. Our findings demonstrated that Fer-1 treatment effectively reversed Micheliolide-induced increases in intra-

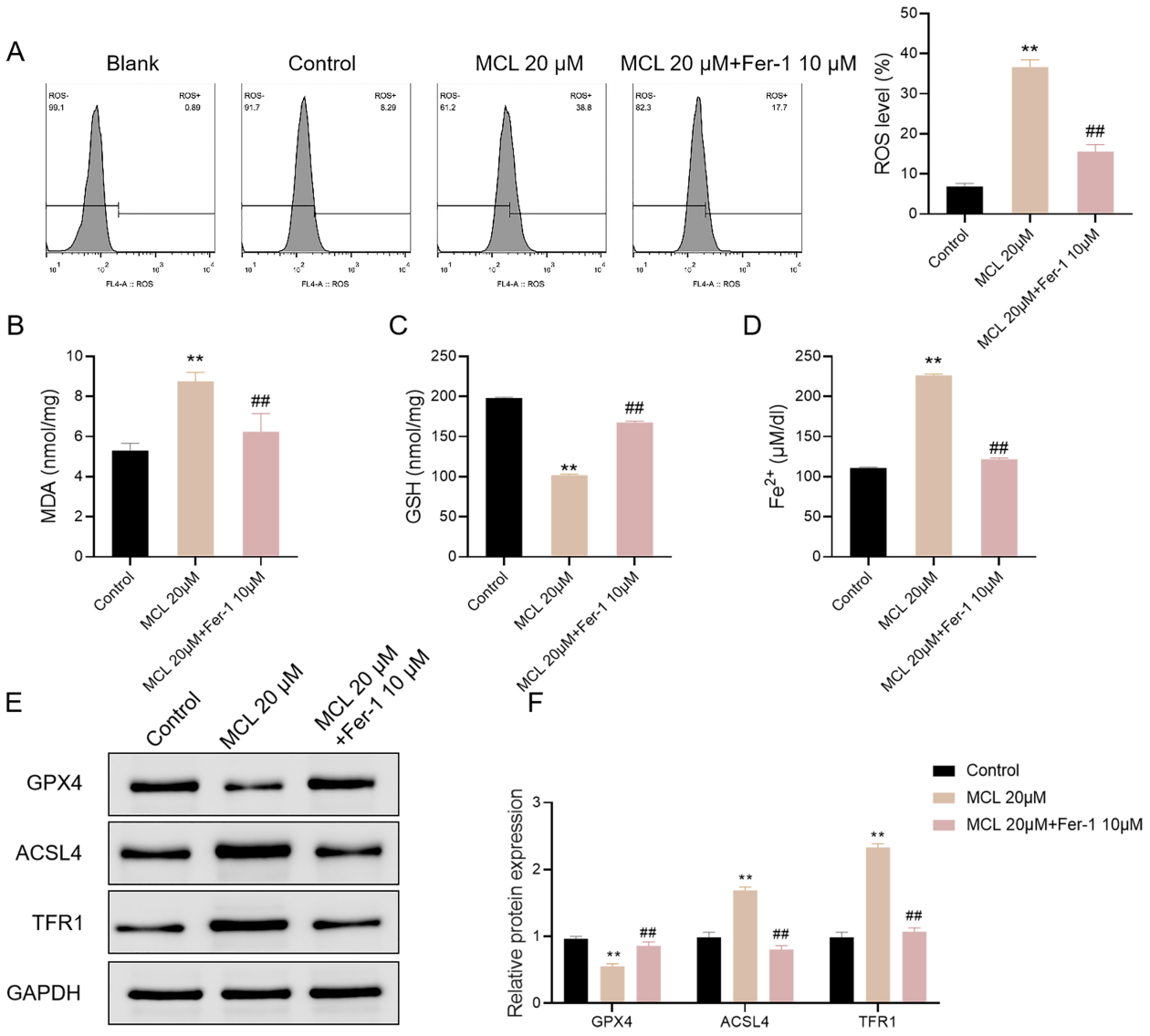

Fig. 2. Micheliolide promotes ferroptosis in NSCLC. DCFH-DA staining was utilized to assess intracellular ROS production (A). Levels of MDA (B), GSH (C), Fe^{2+} (D), GPX4, ACSL4, and TFR1 protein, as well as their activity levels in H1299 cells (E,F), were depicted. All data were expressed as mean ± standard deviation (SD). $^{**}p < 0.01$ indicated comparison with the Control; $^{\#\#}p < 0.01$ indicated comparison with MCL. Each experiment was independently repeated three times (n = 3). NSCLC, non-small cell lung cancer; DCFH-DA, 2′,7′-Dichlorodihydrofluorescein diacetate; ACSL4, Acyl-CoA Synthetase Long-Chain Family Member 4; TFR1, Transferrin Receptor 1; GAPDH, Glyceraldehyde-3-phosphate dehydrogenase; ROS, reactive oxygen species; MDA, malondialdehyde; GSH, glutathione; GPX4, glutathione peroxidase 4; Fer-1, ferrostatin-1.

cellular iron and ROS levels, as well as the decrease in GPX4 expression, in H1299 cells. These results strongly support that ferroptosis is the primary mechanism underlying Micheliolide-induced cytotoxic effect in NSCLC cells.

To further validate the role of Nrf2 signaling in Micheliolide-induced ferroptosis, NSCLC cells were pre-treated with a specific Nrf2 activator, tBHQ. The tBHQ prevents ferroptosis by reducing iron levels and suppressing lipid peroxidation. Interestingly, pre-treatment with tBHQ effectively restored Nrf2 expression and activity, resulting in significantly reduced levels of ROS, lipid peroxidation, and intracellular iron [29]. Consequently, tBHQ pre-treatment significantly enhanced cell viability and attenuated Micheliolide-induced ferroptosis. These findings underscore the protective role of Nrf2 signaling in safeguarding cells from ferroptosis, highlighting that Nrf2 activators could serve as valuable adjuvants to enhance the therapeutic efficacy of ferroptosis inducers such as Micheliolide.

Overall, this study provides compelling evidence supporting Micheliolide as a potential ferroptosis inducer for

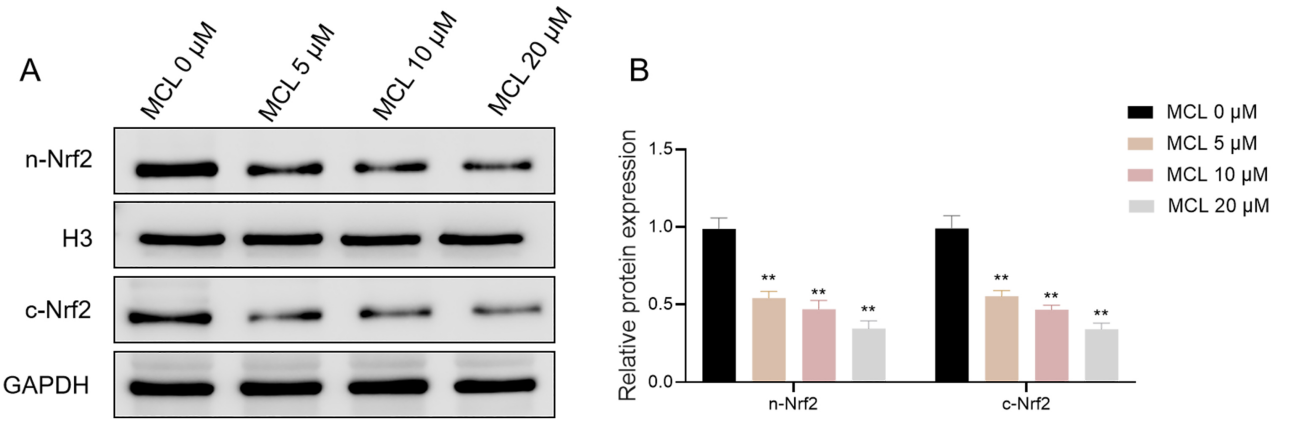

Fig. 3. Micheliolide inhibits Nrf2 pathway activation. (A,B) Western blot analysis of Nrf2 protein levels in both the nucleus (n-Nrf2) and cytoplasm (c-Nrf2) of H1299 cells treated with varying concentrations of Micheliolide (0, 5, 10, and 20 μM) for 24 hours. Relative fold changes compared to the control group (0 μM) were expressed as mean ± SD. ** $p < 0.01$ compared with the 0 μM control group. Each experiment was independently repeated three times (n = 3). Nrf2, nuclear factor erythroid 2-related factor 2.

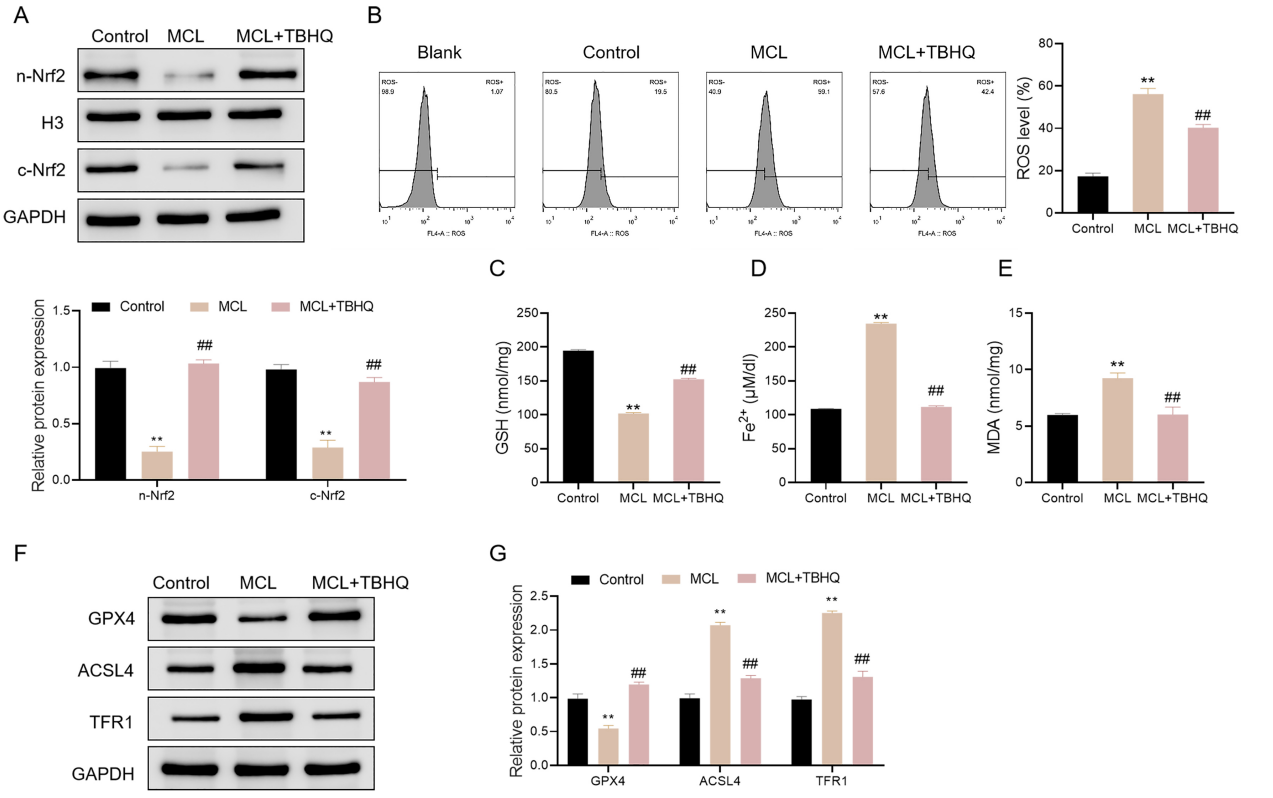

Fig. 4. Nrf2 activation attenuates Micheliolide-induced ferroptosis. (A) Western blot analysis depicting Nrf2 protein levels in both the nucleus (n-Nrf2) and cytoplasm (c-Nrf2) of H1299 cells pre-treated with tBHQ (10 μM) followed by Micheliolide treatment. Relative fold changes compared to the control group are presented as mean ± SD. (B) Levels of reactive oxygen species (ROS), (C) Glutathione (GSH), (D) Fe^{2+}, and (E) malondialdehyde (MDA) in H1299 cells pre-treated with tBHQ followed by Micheliolide treatment. (F,G) GPX4, ACSL4, and TFR1 protein, as well as their activity levels in H1299 cells, were depicted. Data were expressed as mean ± SD. **$p < 0.01$ compared to the control group; $^{\#\#}$ $p < 0.01$ compared to the MCL group. Each experiment was independently repeated three times (n = 3). tBHQ, tert-butylhydroquinone.

NSCLC therapy. By targeting the Nrf2 signaling pathway, Micheliolide can circumvent the antioxidant defense mechanisms of cancer cells, leading to iron-mediated cell death. This novel therapeutic approach holds promise for overcoming therapy resistance in NSCLC and improving treatment outcomes.

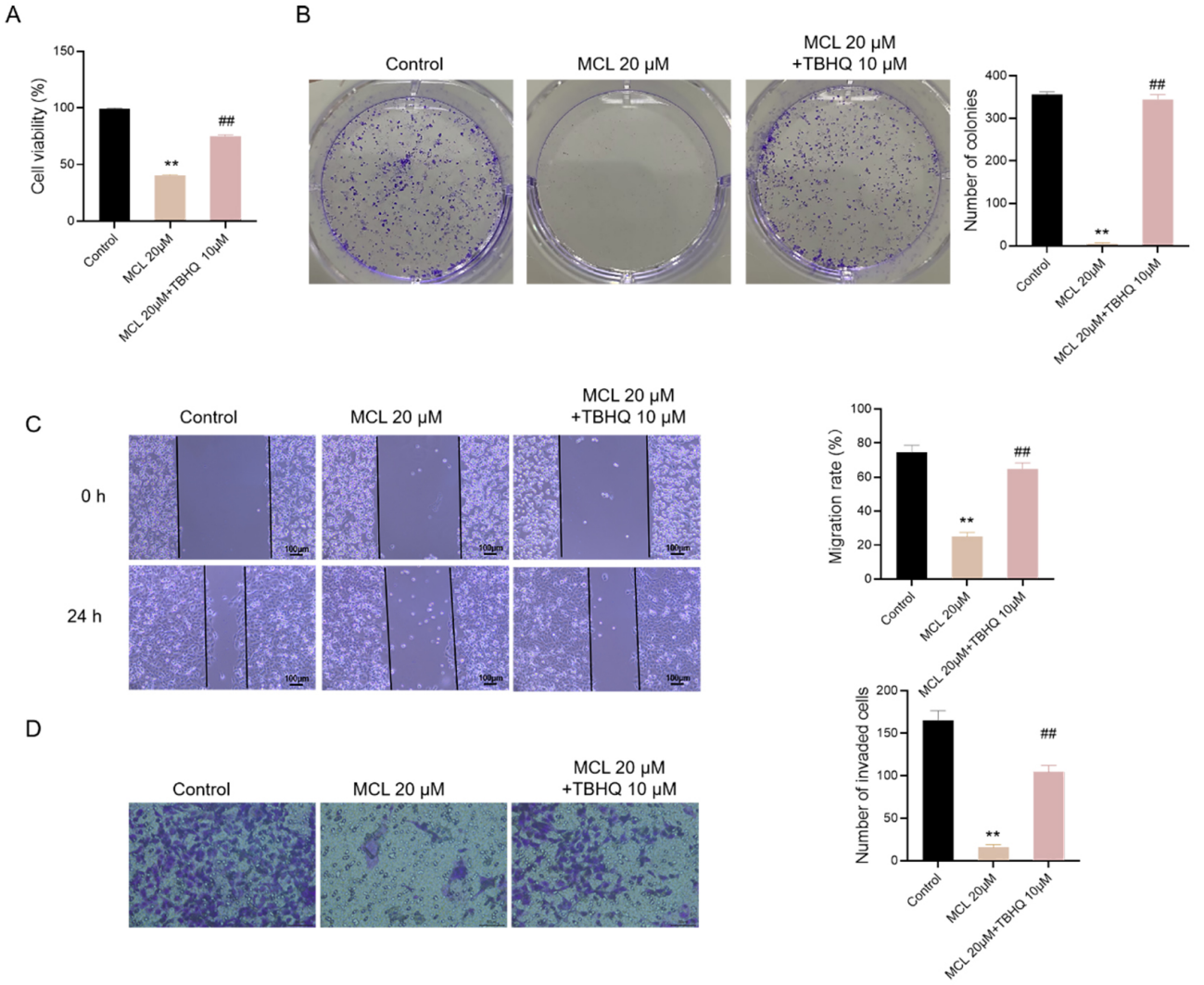

Fig. 5. Nrf2 activation mitigates the inhibitory effects of Micheliolide on NSCLC cells. Cell viability was assessed using the CCK-8 assay (A), proliferation ability was evaluated using colony the formation assay (B), and migration and invasion abilities were determined using the wound healing assay (C) and Transwell assay (D), respectively. Relative fold changes were expressed as mean ± SD. $^{**}p < 0.01$ indicates comparison with control; $^{\#\#}p < 0.01$ indicates comparison with MCL. Each experiment was independently repeated three times (n = 3).

The results show that tBHQ can partially reverse the effects of Micheliolide, underscoring the significant role of the Nrf2 pathway in this process. However, it is likely that additional signaling pathways, such as the Keap1-Nrf2-ARE axis or other antioxidant defense mechanisms, also contribute to the overall effects of Micheliolide, potentially mediating responses that tBHQ alone cannot reverse. In addition to Nrf2 and GPX4, other key regulators of ferroptosis, such as solute carrier family 7 member 11 (SLC7A11) and ferroptosis suppressor protein 1 (FSP1), play an essential role in controlling lipid peroxidation and iron metabolism [30]. Although these factors were not evaluated in the present study, their interaction with the Nrf2-GPX4 axis and modulation by MCL merit further investigation. Moreover, while our findings show that Nrf2 activation can restore cancer cell viability by attenuating ferroptosis, this observation appears paradoxical given Nrf2's well-established roles in promoting tumorigenesis and contributing to drug resistance [27]. This highlights the complex, context-dependent, and cell-type-specific functions of Nrf2, where its activation may confer survival advantages under certain oxidative stresses but also promote cancer progression in others. These dual roles warrant careful mechanistic investigations to understand Nrf2's function and to develop targeted therapeutic strategies that balance its protective and oncogenic effects.

Micheliolide offers a novel therapeutic candidate capable of overcoming such resistance by targeting the Nrf2 signaling pathway and inducing ferroptosis. This approach may substantially enhance cancer treatment effi-

cacy, particularly in patients with advanced or therapy-resistant NSCLC. By inducing ferroptosis, Micheliolide could expand therapeutic possibilities for patients with limited options, thereby improving clinical outcomes. Additionally, further investigation into the molecular mechanisms of Micheliolide-induced ferroptosis and its interaction with other signaling pathways may identify additional therapeutic targets, enhancing the overall effectiveness of this promising anticancer strategy.

Patients with chemotherapy- or radiotherapy-resistant NSCLC, particularly those with p53-deficient tumors, present significant therapeutic challenges due to their increased resistance to conventional treatments [7]. These patients often have limited therapeutic options and face rapid disease progression. Ferroptosis, a form of iron-dependent, non-apoptotic cell death driven by lipid peroxidation, provides a potential alternative to conventional therapies [31]. Unlike apoptosis, ferroptosis functions through p53-independent mechanisms, making it a promising alternative for targeting treatment-resistant cancer cells [10].

In NSCLC cases resistant to chemotherapy or radiotherapy, inducing ferroptosis through agents such as Micheliolide may offer a strategy to circumvent the apoptotic pathway impairments often associated with p53 deficiency [32]. Micheliolide enhances ROS accumulation and lipid peroxidation while inhibiting the Nrf2-GSH-GPX4 antioxidant defense system, thereby promoting ferroptosis and increasing the sensitivity of resistant cancer cells to therapeutic intervention. By diminishing the antioxidant mechanisms that p53-deficient and treatment-resistant tumors rely on, Micheliolide's ability to induce ferroptosis could represent a novel and effective approach to overcome resistance and improve outcomes in advanced NSCLC [12].

Despite the promising findings, this study has several limitations. First, all experiments were conducted using a single NSCLC cell line (H1299), which may not reflect the full molecular diversity of NSCLC. Validation in additional cell models, including adenocarcinoma and squamous cell carcinoma models, is necessary to improve the generalizability of the findings. Second, although the role of Nrf2 was investigated using the pharmacological activator tBHQ, no genetic approaches such as siRNA or CRISPR-Cas9-mediated editing were employed to confirm its specific involvement. Moreover, tBHQ may influence other redox-sensitive pathways, potentially introducing confounding effects. Third, potential upstream or parallel pathways, including the Keap1-Nrf2-ARE axis and Phosphoinositide 3-kinase (PI3K)/Protein kinase B (Akt) signaling, were not examined. Finally, this study lacks *in vivo* experiments, leaving the pharmacokinetics, safety profile, and therapeutic efficacy of Micheliolide unaddressed. To maximize clinical benefits, future studies should address these limitations and explore their potential in combination with standard therapies, such as Epidermal Growth Factor Receptor (EGFR) inhibitors or immunotherapy.

Conclusions

In conclusion, Micheliolide demonstrates strong potential as a promising anticancer agent by inducing ferroptosis in NSCLC cells through modulation of the Nrf2 signaling pathway. This study emphasizes the therapeutic potential of Micheliolide-based therapies in NSCLC and underscores the significance of further investigation to support their clinical application. The development of ferroptosis-inducing agents like Micheliolide offers a novel and promising therapeutic approach for combating NSCLC and possibly other resistant malignancies.

Availability of Data and Materials

The data used to support the findings of this study are available from the corresponding author upon request.

Author Contributions

Study concept and design: HL, TFQ; Analysis and interpretation of data: HL, QYX; Drafting of the manuscript: HL, QYX; Critical revision of the manuscript for important intellectual content: HL, QYX, TFQ; Study supervision: all authors. All authors have read and approved the manuscript. All authors have participated sufficiently in the work and agreed to be accountable for all aspects of the work.

Ethics Approval and Consent to Participate

Not applicable.

Acknowledgment

Not applicable.

Funding

This research received no external funding.

Conflict of Interest

The authors declare no conflict of interest.

References

[1] Sung H, Ferlay J, Siegel RL, Laversanne M, Soerjomataram I, Jemal A, *et al*. Global Cancer Statistics 2020: GLOBOCAN Estimates of Incidence and Mortality Worldwide for 36 Cancers in 185 Countries. CA: a Cancer Journal for Clinicians. 2021; 71: 209–249. https://doi.org/10.3322/caac.21660.

[2] Ettinger DS, Wood DE, Aisner DL, Akerley W, Bauman JR, Bharat A, *et al*. Non-Small Cell Lung Cancer, Version 3.2022, NCCN Clinical Practice Guidelines in Oncology. Journal of the National Comprehensive Cancer Network: JNCCN. 2022; 20: 497–530. https://doi.org/10.6004/jnccn.2022.0025.

[3] Yang SR, Schultheis AM, Yu H, Mandelker D, Ladanyi M, Büttner R. Precision medicine in non-small cell lung cancer: Cur-

rent applications and future directions. Seminars in Cancer Biology. 2022; 84: 184–198. https://doi.org/10.1016/j.semcancer.2020.07.009.

[4] Srivastava S, Mohanty A, Nam A, Singhal S, Salgia R. Chemokines and NSCLC: Emerging role in prognosis, heterogeneity, and therapeutics. Seminars in Cancer Biology. 2022; 86: 233–246. https://doi.org/10.1016/j.semcancer.2022.06.010.

[5] Hadian K, Stockwell BR. SnapShot: Ferroptosis. Cell. 2020; 181: 1188–1188.e1. https://doi.org/10.1016/j.cell.2020.04.039.

[6] Yao X, Li W, Fang D, Xiao C, Wu X, Li M, *et al*. Emerging Roles of Energy Metabolism in Ferroptosis Regulation of Tumor Cells. Advanced Science (Weinheim, Baden-Wurttemberg, Germany). 2021; 8: e2100997. https://doi.org/10.1002/advs.202100997.

[7] Tang D, Chen X, Kang R, Kroemer G. Ferroptosis: molecular mechanisms and health implications. Cell Research. 2021; 31: 107–125. https://doi.org/10.1038/s41422-020-00441-1.

[8] Wu K, El Zowalaty AE, Sayin VI, Papagiannakopoulos T. The pleiotropic functions of reactive oxygen species in cancer. Nature Cancer. 2024; 5: 384–399. https://doi.org/10.1038/s43018-024-00738-9.

[9] Tate EW, Soday L, de la Lastra AL, Wang M, Lin H. Protein lipidation in cancer: mechanisms, dysregulation and emerging drug targets. Nature Reviews. Cancer. 2024; 24: 240–260. https://doi.org/10.1038/s41568-024-00666-x.

[10] Lei G, Zhuang L, Gan B. Targeting ferroptosis as a vulnerability in cancer. Nature reviews. Cancer. 2022; 22: 381–396. https://doi.org/10.1038/s41568-022-00459-0.

[11] Hassannia B, Vandenabeele P, Vanden Berghe T. Targeting Ferroptosis to Iron Out Cancer. Cancer Cell. 2019; 35: 830–849. https://doi.org/10.1016/j.ccell.2019.04.002.

[12] Gao X, Su Q, Pan H, You Y, Ruan Z, Wu Y, *et al*. Arsenic-Induced Ferroptosis in Chicken Hepatocytes via the Mitochondrial ROS Pathway. Biological trace element research. 2024; 202: 4180–4190. https://doi.org/10.1007/s12011-023-03968-7.

[13] Yang WS, SriRamaratnam R, Welsch ME, Shimada K, Skouta R, Viswanathan VS, *et al*. Regulation of ferroptotic cancer cell death by GPX4. Cell. 2014; 156: 317–331. https://doi.org/10.1016/j.cell.2013.12.010.

[14] Li S, Zheng L, Zhang J, Liu X, Wu Z. Inhibition of ferroptosis by up-regulating Nrf2 delayed the progression of diabetic nephropathy. Free Radical Biology & Medicine. 2021; 162: 435–449. https://doi.org/10.1016/j.freeradbiomed.2020.10.323.

[15] Kerins MJ, Ooi A. The Roles of NRF2 in Modulating Cellular Iron Homeostasis. Antioxidants & Redox Signaling. 2018; 29: 1756–1773. https://doi.org/10.1089/ars.2017.7176.

[16] Ursini F, Maiorino M. Lipid peroxidation and ferroptosis: The role of GSH and GPx4. Free Radical Biology & Medicine. 2020; 152: 175–185. https://doi.org/10.1016/j.freeradbiomed.2020.02.027.

[17] Xu Y, Li Y, Li J, Chen W. Ethyl carbamate triggers ferroptosis in liver through inhibiting GSH synthesis and suppressing Nrf2 activation. Redox Biology. 2022; 53: 102349. https://doi.org/10.1016/j.redox.2022.102349.

[18] Li J, Li S, Guo J, Li Q, Long J, Ma C, *et al*. Natural Product Micheliolide (MCL) Irreversibly Activates Pyruvate Kinase M2 and Suppresses Leukemia. Journal of Medicinal Chemistry. 2018; 61: 4155–4164. https://doi.org/10.1021/acs.jmedchem.8b00241.

[19] Jia Y, Zhang C, Zhou L, Xu H, Shi Y, Tong Z. Micheliolide overcomes KLF4-mediated cisplatin resistance in breast cancer cells by downregulating glutathione. OncoTargets and Therapy. 2015; 8: 2319–2327. https://doi.org/10.2147/OTT.S88661.

[20] Viennois E, Xiao B, Ayyadurai S, Wang L, Wang PG, Zhang Q, *et al*. Micheliolide, a new sesquiterpene lactone that inhibits intestinal inflammation and colitis-associated cancer. Laboratory Investigation; a Journal of Technical Methods and Pathology. 2014; 94: 950–965. https://doi.org/10.1038/labinvest.2014.89.

[21] Kong P, Yu KN, Yang M, Almahi WA, Nie L, Chen G, *et al*. Micheliolide Enhances Radiosensitivities of p53-Deficient Non-Small-Cell Lung Cancer via Promoting HIF-1α Degradation. International Journal of Molecular Sciences. 2020; 21: 3392. https://doi.org/10.3390/ijms21093392.

[22] Franken NAP, Rodermond HM, Stap J, Haveman J, van Bree C. Clonogenic assay of cells in vitro. Nature Protocols. 2006; 1: 2315–2319. https://doi.org/10.1038/nprot.2006.339.

[23] Tang D, Kang R, Berghe TV, Vandenabeele P, Kroemer G. The molecular machinery of regulated cell death. Cell Research. 2019; 29: 347–364. https://doi.org/10.1038/s41422-019-0164-5.

[24] Xu Z, Xu J, Sun S, Lin W, Li Y, Lu Q, *et al*. Mecheliolide elicits ROS-mediated ERS driven immunogenic cell death in hepatocellular carcinoma. Redox Biology. 2022; 54: 102351. https://doi.org/10.1016/j.redox.2022.102351.

[25] Liu J, Yang G, Zhang H. Glyphosate-triggered hepatocyte ferroptosis via suppressing Nrf2/GSH/GPX4 axis exacerbates hepatotoxicity. The Science of the Total Environment. 2023; 862: 160839. https://doi.org/10.1016/j.scitotenv.2022.160839.

[26] Llovet JM, Pinyol R, Yarchoan M, Singal AG, Marron TU, Schwartz M, *et al*. Adjuvant and neoadjuvant immunotherapies in hepatocellular carcinoma. Nature Reviews. Clinical Oncology. 2024; 21: 294–311. https://doi.org/10.1038/s41571-024-00868-0.

[27] Tang X, Wang H, Fan L, Wu X, Xin A, Ren H, *et al*. Luteolin inhibits Nrf2 leading to negative regulation of the Nrf2/ARE pathway and sensitization of human lung carcinoma A549 cells to therapeutic drugs. Free Radical Biology & Medicine. 2011; 50: 1599–1609. https://doi.org/10.1016/j.freeradbiomed.2011.03.008.

[28] Dixon SJ, Lemberg KM, Lamprecht MR, Skouta R, Zaitsev EM, Gleason CE, *et al*. Ferroptosis: an iron-dependent form of nonapoptotic cell death. Cell. 2012; 149: 1060–1072. https://doi.org/10.1016/j.cell.2012.03.042.

[29] Wang Q, Bin C, Xue Q, Gao Q, Huang A, Wang K, *et al*. GSTZ1 sensitizes hepatocellular carcinoma cells to sorafenib-induced ferroptosis via inhibition of NRF2/GPX4 axis. Cell Death & Disease. 2021; 12: 426. https://doi.org/10.1038/s41419-021-03718-4.

[30] Doll S, Freitas FP, Shah R, Aldrovandi M, da Silva MC, Ingold I, *et al*. FSP1 is a glutathione-independent ferroptosis suppressor. Nature. 2019; 575: 693–698. https://doi.org/10.1038/s41586-019-1707-0.

[31] Jennis M, Kung CP, Basu S, Budina-Kolomets A, Leu JIJ, Khaku S, *et al*. An African-specific polymorphism in the TP53 gene impairs p53 tumor suppressor function in a mouse model. Genes & Development. 2016; 30: 918–930. https://doi.org/10.1101/gad.275891.115.

[32] Ou Y, Wang SJ, Li D, Chu B, Gu W. Activation of SAT1 engages polyamine metabolism with p53-mediated ferroptotic responses. Proceedings of the National Academy of Sciences of the United States of America. 2016; 113: E6806–E6812. https://doi.org/10.1073/pnas.1607152113.